Colloidal assemblies on patterned silane layers

Ulrich Jonas*, Aránzazu del Campo, Christian Krüger, Gunnar Glasser, and Diana Boos

Max Planck Institute for Polymer Research, Ackermannweg 10, 55128 Mainz, Germany

Edited by Jack Halpern, University of Chicago, Chicago, IL, and approved February 19, 2002 (received for review November 29, 2001)

The site-selective assembly of colloidal polymer particles onto laterally patterned silane layers was studied as a model system for the object assembly process at mesoscale dimensions. The structured silane monolayers on silicon oxide substrates were fabricated by a combination of liquid- and gas-phase deposition of different trialkoxysilanes with a photolithographic patterning technique. By using this method various types of surface functionalizations such as regions with amino functions next to areas of the bare silica surface or positively charged regions of a quaternary ammonium silane surrounded by a hydrophobic octadecylsilane film could be obtained. Furthermore, a triethoxysilane with a photoprotected amino group was synthesized, which allowed direct photopatterning after monolayer preparation, leading to free NH_2 groups at the irradiated regions. The different silane monolayer patterns were used to study the surface assembly behavior of carboxylated methacrylate particles by optical and scanning electron microscopy. In dependence of the assembly conditions (different surface functionalizations, pH, and drying conditions), a selective preference of the particles for a specific surface type versus others was found. Site-specific colloid adsorption could be observed also on the photosensitive silane layers after local deprotection with light. From the photosensitive silane and positively charged ammonium silane, molecularly mixed monolayers were prepared, which allowed particle adsorption and photoactivation within the same monolayer as shown by fluorescence labeling.

One of the major driving forces in modern technology is based on the desire for miniaturization, which leads to smaller and lighter devices and a higher number of functional units per volume element. This tendency is prevalent particularly in microelectronics, optics, and sensors. Fabrication methods for small parts and structuring techniques have been developed very far, entering now the regime of nanoscopic dimensions (1, 2). Integrating individual objects of such dimensions into more complex structures and devices, on the other hand, represents a key challenge. Especially for the interfacing of nanoscopic devices with the macroscopic world, a large number of hierarchical organization levels are required to be implemented and controlled to actually use such small devices. One strategy toward attaining this goal emerges from the application of self-organization and assembly concepts that are ubiquitously present in the biological world and used successfully in supramolecular chemistry. Based on these principles several methods for the assembly of objects into two- and three-dimensional structures have been demonstrated at length scales from several nanometers up to millimeters (3–11). Most of these methods rely on shape complementarity of the objects, the surface tension at the interface of an auxiliary liquid and the object surfaces, and specific molecular interactions between the individual objects.

A refined strategy for the assembly of mesoscale objects is presented in Fig. 1, consisting of a three-step procedure. In the first step molecular layers (A, A', B, and B') are deposited at specific sites onto the objects. These layers carry functional groups that can form reversible attractive interactions with complementary surface layers on opposing objects (such as A and A' or B and B'), which defines how parts interact in a desired spacial orientation. In the second step the modified objects are brought together in a favorable environment to allow reversible assembly and positioning under the control of the surface layers. To stabilize the obtained assembly structure functional groups in the surface permanently, layers are activated by an external stimulus (e.g., light or heat) in the third step, which induces the formation of covalent bonds between neighboring objects. Based on this procedure the molecular layers have to be composed of two functional entities: first, the component that does form reversible attractive interactions and which we might call alignment markers, and second, the species that can be activated to induce chemical bonding and to which we refer as molecular glue.

A convenient system for the study of fundamental issues related to the described object-assembly method consists of patterned molecular layers on planar substrates and colloidal particles as model objects with mesoscale dimensions. The resulting structured surfaces can show a variety of interesting properties such as superhydrophobicity (12), antireflectivity (13), and self-cleaning behavior (14) with many possible applications ranging from electromechanical devices (15) over microfluidics (16) and separation technology (17) to bio- and chemosensors (18).

Polymer colloids are particularly interesting as model objects (19), because such particles can be made of a large variety of different polymers with diameters ranging from several nanometers up to many micrometers, whereas their surface chemistry and charge can be controlled by the monomer composition in a later stage of particle preparation. For this particular study polybutylmethacrylate (PBMA) particles with carboxylic acid surface functions were synthesized by emulsion polymerization (20). In the literature several methods for the physical adsorption of colloidal particles with 100-nm to millimeter dimensions onto unpatterned substrates that rely on intrinsic properties of the particles and surfaces (such as electrostatic attraction) are reported (ref. 21 and references therein). Much less work is reported on the chemisorption of such particles (22–24), and only little effort has been directed to the generation of patterned colloid assemblies onto chemically structured monolayers (refs. 25–29; our discussion shall exclude metallic and semiconductor nanoparticles with diameters of only several nanometers). The substrates for these patterned particle deposition experiments were either gold surfaces regiospecifically modified with functionalized thiols by microcontact printing or silica surfaces that were photopatterned with a preadsorbed cationic monomer. In the study by Aizenberg *et al.* (25), the specific effect of capillary forces on the positioning of polystyrene particles (—COOH or amidine functionalized) on charged thiol monolayer patterns was investigated. Hammond and coworkers (27) used polyelectrolyte multilayers on patterned thiol monolayers to adsorb silica and surface-modified polystyrene latex particles (—OSO_3H, —COOH, and —$CONH_2$) in dependence of pH, salt concentration, and the presence of surfactants. In our study we used glass, quartz, and silicon wafers with a native oxide layer as substrates for the particle-assembly experiments. These substrates were modified with patterned silane layers by vapor- and

This paper was submitted directly (Track II) to the PNAS office.

Abbreviations: NVoc silane, [3-(triethoxy-silanyl)-propyl]carbamic acid 4,5-dimethoxy-2-nitrobenzyl ester; PBMA, polybutylmethacrylate; SEM, scanning electron microscope.

*To whom reprint requests should be addressed. E-mail: jonas@mpip-mainz.mpg.de.

www.pnas.org/cgi/doi/10.1073/pnas.082634799

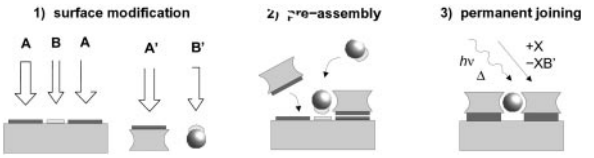

Fig. 1. Schematic outline of the object assembly procedure. (*1*) Local modification of individual objects with molecular surface layers (*A*, *A′*, *B*, and *B′*). (*2*) Preassembly of the modified objects under the control of specific attractions between corresponding surface layers (*A*, *A′*, *B*, and *B′*). (*3*) Permanent fixation of the assembly structure through covalent bond formation between the layers after activation (e.g., by light, heat, or chemical agents).

liquid-phase deposition using photolithography for the patterning process (30). The procedure yielded reactive or charged surface regions next to hydrophilic or inert hydrophobic areas.

Materials and Methods

Synthesis of [3-(Triethoxy-silanyl)-propyl]carbamic acid 4,5-dimethoxy-2-nitrobenzyl Ester (NVoc Silane). The photoprotected aminosilane (NVoc structure, see Fig. 4) was synthesized in a two-step procedure starting from allylamine and 6-nitroveratryloxycarbonyl chloride (both from Fluka), which yielded after reaction under Schotten–Baumann conditions the corresponding urethane (31). The triethoxysilyl function then was introduced into the allyl double bond by hydrosilylation with triethoxysilane at 80°C in an inert atmosphere (N_2) using H_2PtCl_6 as catalyst (32). The reaction product was purified by column chromatography on hexamethyldisilazane-passivated silica gel. Details of the synthesis and characterization for this and related silane derivatives will be reported elsewhere.

Photodeprotection of NVoc Silane-Coated Substrates. The NVoc protecting group could be removed selectively from the substrate by irradiation through a gold mask for 30 s with an argon laser (200 mW on a 1-cm^2 area) at 364 nm. The deprotection reaction is a light-induced intramolecular oxidation of the benzylic carbon-hydrogen bond in *ortho* position to the nitro group, which leads to an aromatic aldehyde. To capture the formed aldehyde, which could react with the deprotected amino function, the substrate is immersed in a 55 mM solution of semicarbazide hydrochloride in methanol during irradiation.

Photolithography. The lateral patterning of the substrates was achieved by standard photolithography (33); experimental details are given in *Detailed Description of the Photolithography Process*, which is published as supporting information on the PNAS web site, www.pnas.org.

Silanization. Solution and vapor-phase silanization were achieved according to previously published procedures (20, 29). Experimental details and characterization data are given in *Detailed Experimental Preparation Procedures and Characterization Data for the Silane Layers*, which is published as supporting information on the PNAS web site.

Fluorescence Labeling and Microscopy of NVoc Silane Layers. To prove the presence of free amino groups at the NVoc silane surface after photodeprotection, the substrates were modified with a commercial fluorescence reagent (Alexa Fluor 488, Molecular Probes) and then imaged by fluorescence microscopy. For this purpose the substrates were incubated for 2–10 h in a 1 mM DMSO solution of the fluorescence label (a hydroxysuccinimide ester), which bound specifically to the free amino functions at the irradiated regions and lead to bright fluorescence in the microscope (Axioskop, Zeiss) (filter set: excitation, 450–490 nm; beam splitter, 510 nm; emission, >515 nm).

Particle Synthesis. The PBMA particles with carboxylic acid surface functions (PBMA—COOH) were synthesized by seeded semicontinuous emulsion polymerization under monomer-starved conditions as reported previously (20). The particles had a diameter of 217 nm (determined by dynamic light scattering) and a negative surface-charge density of 2 nm^2 per charge (polyelectrolyte titration under shear flow).

Particle Assembly Procedures. For the particle assembly experiments the patterned substrates either were immersed completely into a latex suspension with 0.1–5% solid content ("dip-coating" procedure) or a droplet of the suspension was placed onto the horizontal substrate ("drop-coating" method) and covered to prevent evaporation. After incubation for several hours (2–12 h), the substrates were washed with water and dried.

Results

Silicon and silicon dioxide are highly relevant materials in many technological areas such as the semiconductor industry and optical signal processing. The surfaces of these materials can be modified specifically with robust and covalently bound silane layers that might carry charged substituents or functional groups for further chemical reactions (34). We have deposited triethoxy- and trimethoxysilanes via the vapor and liquid phase onto substrates that were covered partially with a resist pattern after photolithographic processing. This method was optimized carefully to yield smooth silane monolayers with regions covered by either octadecyl, aminopropyl, or trimethylammonium propyl functions next to free silica surface areas. The monolayer structure and quality was characterized in detail by scanning force microscopy, scanning electron microscopy, optical microscopy after water condensation, ellipsometry, and water contact angle measurements as reported previously (refs. 20 and 29; see *Detailed Experimental Preparation Procedures and Characterization Data for the Silane Layers*). The careful optimization of reaction conditions was necessary, because the chemistry of trialkoxysilane hydrolysis and adsorption to silica surfaces is a complex multistep process of hydrolytic alkoxysilyl bond cleavage, silanol condensation in solution, adsorption of monomeric and oligomeric species to the surface, silanol condensation at the surface, and chemical bonding to surface silanol groups. All these concurrent processes can lead rapidly to undesired three-dimensional aggregates on the substrate. In comparison, vapor-phase deposition of octadecyltriethoxysilane led directly to well defined monolayers, because hydrolysis, condensation, and bonding occur exclusively at the substrate surface.

The assembly behavior of PBMA particles with carboxylic surface groups (PBMA—COOH) was studied on these patterned substrates in dependence of the pH. The particles with a diameter of 217 nm and a surface-charge density of 2 nm^2 per charge were washed thoroughly with pure water before the experiments to remove excess ions or surfactants. Fig. 2 shows the optical micrographs and scanning electron microscope (SEM) images of the dried assembly structures prepared at different pH values on an amino-functionalized substrate with free silica regions. At pH 4.5 the substrate is covered completely with a particle submonolayer, and a slight preference of adsorption for the silanol versus the amino surface can be distinguished (Fig. 2 *a* and *d*). The particle density on the amino surface is 6.93 ± 0.33 particles per μm^2 and 7.44 ± 0.22 particles per μm^2 on the silanol surface. On a substrate pattern with trimethylammonium and silanol regions, a similar assembly behavior is observed for PBMA—COOH at pH 4.5 with the whole surface being covered homogeneously by a particle layer (7.5 ± 1 particles per μm^2). This pH value lies below the pKa value of polyacrylic acid (pKa ≈ 5; ref. 27), thus most of the carboxylic acid functions on the PBMA—COOH particles are not dissociated, and only a low surface charge is to be expected. The silica

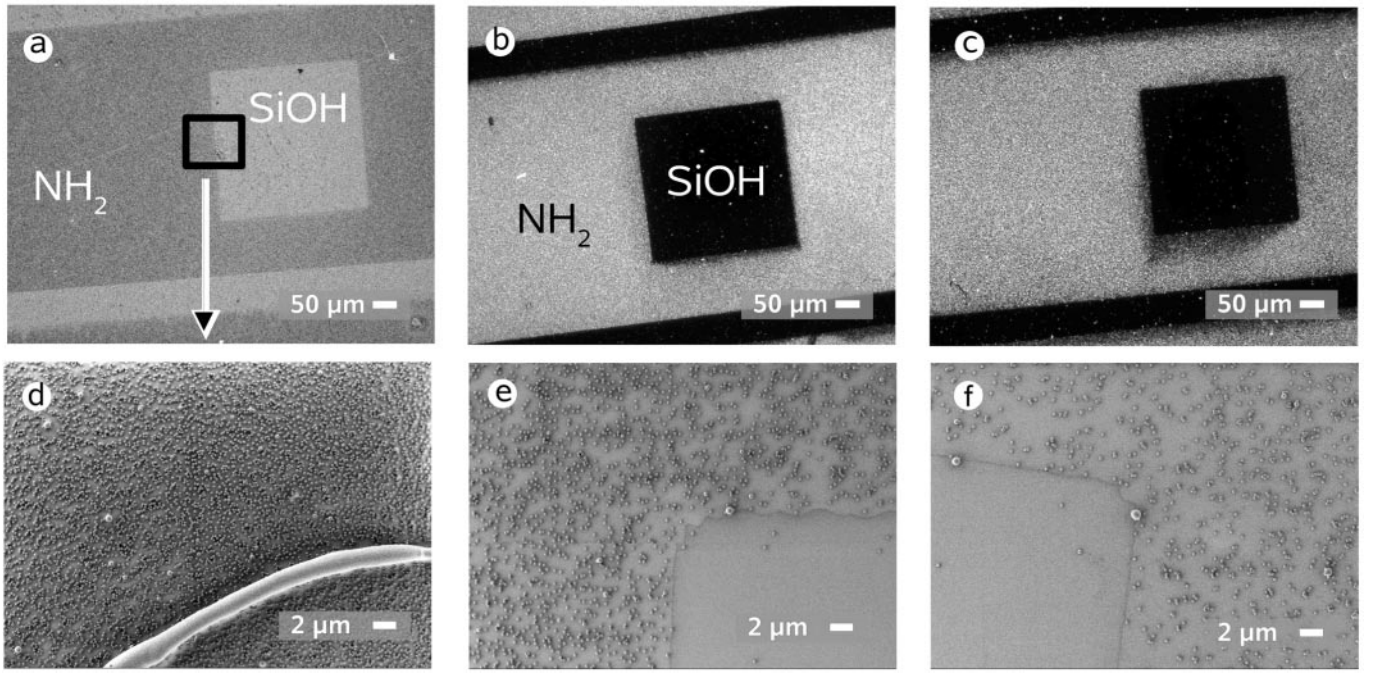

Fig. 2. Optical micrographs (dark field, *a–c*) and corresponding SEM images (*d–f*) of carboxylated PBMA particles (217 nm) assembled onto an aminopropylsilane monolayer pattern with free silica regions (SiOH square and stripes). Assembly pH: 4.5 (*a* and *d*), 7.0 (*b* and *e*), 9.0 (*c* and *f*).

surface at this pH is weakly dissociated, bearing only a small negative charge (35); therefore the particle adsorption should be driven mostly by polar interactions (such as hydrogen bonding) with electrostatic effects playing a minor role. This explanation is supported by the little difference in particle densities found on the various surface types. When the assembly is conducted at pH 7.0, a drastic change of adsorption selectivity of the particles for the amino and ammonium surface is observed (Fig. 2 *b* and *e*), whereas almost no particles adhere to the silica surface. This selectivity can be explained by electrostatic attraction of the now negatively charged polymer particles to the positively charged amino and ammonium regions and the Coulomb repulsion between the like-charged colloids and silica surface. The negative charge on the particles is responsible also for interparticle repulsion leading to lower surface coverage (amino, 2.41 ± 0.67 particles per μm^2; ammonium, 0.94 ± 0.13 particles per μm^2) than at pH 4.5. At an even higher pH of 9.0, the same selectivity of the colloids for the amino and ammonium surfaces is seen (Fig. 2 *c* and *f*) along with a further reduction in particle density (amino, 1.48 ± 0.19 particles per μm^2; ammonium, 0.59 ± 0.34 particles per μm^2) caused by the increased negative particle charge. When comparing the particle densities between amino and ammonium substrates at pH 7.0 and 9.0, more particles are found on the amino surface under identical assembly conditions, which could be caused by either a different number of surface groups (more amino than ammonium functions per surface unit) or different interactions between the amino and carboxylic acid moieties compared with ammonium and acid groups. From the monolayer characterization (thickness, morphology) both types of silane layers are very similar, and thus no major difference in silane and head-group density is expected. From a simple molecular model of the aminopropylsilane, the surface density is ≈0.2 nm^2 per amino group, which is in correspondence with values from the literature (36, 37). On the other hand, the neutral amino group can be protonated below approximately pH 9.0, which leads to a positive charge at the surface. The equilibrium of protonation and charge density will strongly depend on the proton concentration and local environment of the silane surface. Thus a carboxylated particle in close proximity to the aminosilane layer can interact through the solvent via electrostatic forces between a solvated carboxy anion and a protonated amino cation as well as by forming a salt pair or a hydrogen bond of a COOH group in direct contact with an amino head group. In principle, covalent amide bond formation between the groups is possible also, which would eliminate local surface charges, but this process is less probable without activation. The silane layers with trimethylammonium head groups carry a permanent charge that is invariable to pH changes. Only the concentration of dissolved ions in the diffuse layer close to the surface and between particles can change with the pH, and thus acid protons from the particles can diffuse with the chloride anions of the ammonium head groups away from the particles into the bulk of the solution. By this process the local charge on the particles would increase and lead to a stronger interparticle repulsion with lower surface coverage compared with the amino surface. Preliminary experiments above pH 9.0 indicate that the particle density on the silica surface seems to increase again. These investigations are complicated by the fact that the Si—O bonds can be hydrolyzed at such high pH and the silane monolayers deteriorate.

Besides specific interactions between the particles and the substrate surface that influence the assembly process in suspension, forces at the triple interface air–liquid–solid (substrate and particles) during liquid retraction and drying have a substantial effect on the organization of the particles (25, 38, 39). Such capillary forces result from the surface tension of the suspending medium. Fig. 3*a* shows the shape of the liquid front formed by a droplet of the colloid suspension that rests on a pattern of trimethylammonium silane squares (≈40 μm wide) in an octadecylsilane matrix. The various particle structures in Fig. 3 *b*, *c*, and *d* result from different liquid retraction velocities on this substrate by slow evaporation of the suspension versus fast removal by pipetting (see *Experimental Procedure for Colloid Assembly with Capillary Forces*, which is published as supporting information on the PNAS web site). Because of different polarities of the hydrophobic octadecyl surface and hydrophilic

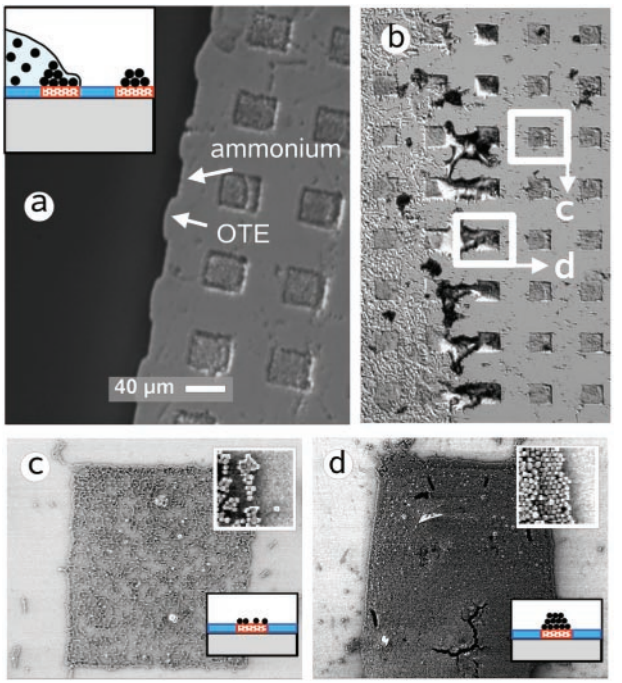

Fig. 3. Optical micrographs (difference interference contrast) of the drying front of a latex suspension droplet on an ammonium silane (squares)/octadecylsilane monolayer pattern before (*a*) and after (*b*) removal of the liquid (*Inset*) Schematic side view of a resting droplet on the substrate. The SEM images show a particle submonolayer on the ammonium pattern formed by electrostatic assembly in suspension (*c*, after rapid removal of the suspension liquid) and a colloid multilayer on a similar pattern generated by capillary forces at the slow-moving drying front (*d*, 0.5 μm·s^{-1}). The magnified insets (3×3 μm^2) and schematics in *c* and *d* show the individual particles of the submonolayer and multilayer, respectively. OTE, octadecyltriethoxysilane.

ammonium regions, pinning of the aqueous suspension over the cationic surface occurs, whereas the liquid is repelled from the alkyl regions (marked by arrows in Fig. 3*a*). This effect leads to an undulated liquid front when the suspension is moving from the right (bright region of substrate in Fig. 3*a*) to the left (dark region of suspension in Fig. 3*a*) with the water adhering to the ammonium layer and forming a low contact angle. On the hydrophobic regions with large contact angles, dewetting occurs and the front moves faster to the left, causing the visible indentations.

If a droplet of the colloid suspension is drying slowly on an unpatterned polar surface (such as silica), the particles aggregate at the rim of the droplet because of attractive capillary forces between the particles when the water film thickness is in the dimension of the particle diameter (38, 39). This effect also takes place when the suspension front is moving slowly over the silane layer pattern ($\approx$0.5 μm·s^{-1} during evaporation) and leads to particle multilayers over the ammonium region. Such multilayer structures at the drying front are shown in Fig. 3*b* after removal of the suspension droplet. The mechanism for the multilayer formation can be explained as follows. First, a submonolayer of electrostatically adsorbed particles forms on the positively charged ammonium pattern in the bulk phase of the suspension (as seen in Fig. 3*c*). The submonolayer coverage is caused by Coulomb repulsion of the like-charged particles, which prevents dense packing in the aqueous medium. Second, during evaporation of the suspension the liquid front moves very slowly over the adsorbed particle layer, and a thin water meniscus remains over the particle assembly, which generates attractive capillary forces between the particles. Because of the slow-moving droplet front, particles from the suspension do

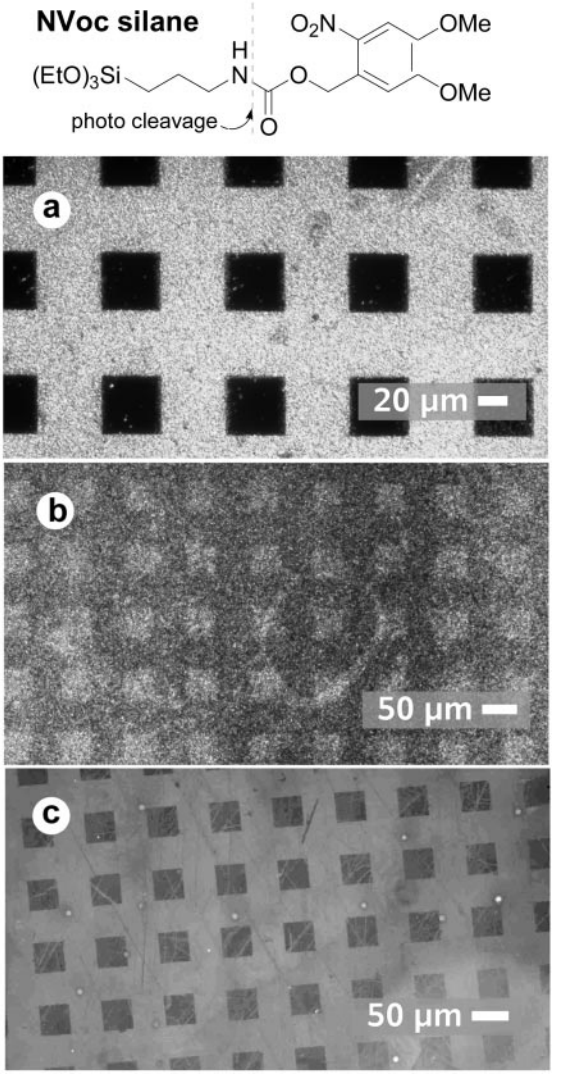

Fig. 4. (*a*) Optical micrograph of latex particles assembled at pH 4.5 onto an NVoc silane monolayer after photodeprotection with an argon laser (364 nm) through a gold mask on quartz (dark squares were protected from light). (*b*) Particle assembly (pH 4.5) on a mixed monolayer of the NVoc and ammonium silane after irradiation (similar to *a*). Bright squares were protected from light and show a lower particle density in the SEM. (*c*) Fluorescence micrograph of a mixed monolayer (NVoc and ammonium silane, similar to *b*) after irradiation and staining with a fluorescent probe (Alexa Fluor 488).

have time to migrate into the thin liquid film at the drying front and aggregate into multilayers over the colloid assembly pattern driven by capillary forces. SEM micrographs of the particle submonolayer (formed at high retraction speed of the suspension, $\approx$1 mm·s^{-1}) and a multilayer (retraction speed $\approx$0.5 μm·s^{-1}) on an ammonium pattern are shown in Fig. 3 *c* and *d*, respectively.

With the described experiments the first two steps of regioselective surface modification and object assembly (as outlined in Fig. 1) could be demonstrated. The next level of refinement involves the integration of the molecular glue entities into the surface layers and their chemical activation. For this purpose a photoprotected aminopropyltriethoxysilane that formed well defined monolayers on silica surfaces was synthesized. We refer to this photosensitive molecule as NVoc silane (Fig. 4). The photolabile protecting group consist of a 6-nitroveratryloxycarbonyl moiety (31) that can be cleaved from the surface with light

at 364 nm (argon laser) in the presence of semicarbazide hydrochloride (as scavenger) to yield a reactive primary amine surface (with the same chemical structure of surface functions as an aminopropyltriethoxysilane monolayer). The existence of free amino groups after deprotection was proven by reaction with a fluorescence label, as discussed further below. Similar photolabile protecting groups have been used for the light-directed synthesis of surface-bound oligopeptide and DNA sequences (40, 41) or for the selective adsorption of metallic and semiconductor nanoparticles (ref. 42 and references 8–11 therein) onto aminopropylsilane surfaces that were modified with nitroveratryloxycarbonyl derivatives. The advantage of synthesizing a silane that directly incorporates a photoprotecting group versus postmodification of an amino surface lies in the simple preparation (one step) of a well defined monolayer structure (all adsorbed silane molecules carry *per se* a protecting group) and the possibility to prepare mixed monolayers with other silane derivatives in arbitrary mixing ratios. Aminopropyltriethoxysilane is very reactive because of the primary amino head group and tends to form undefined three-dimensional aggregates and multilayers from solution if the reaction conditions are not controlled carefully. The protected NVoc silane is much less polar and reactive, which facilitates monolayer preparation. After local deprotection of a pure NVoc silane monolayer by irradiation through a mask (40×40-μm^2 gold squares on quartz), the PBMA—COOH particles selectively assembled onto only the deprotected amino regions at pH 4.5 by polar attraction (3.26 ± 0.44 particles per μm^2, as shown in Fig. 4*a*). No particles were found on the hydrophobic areas of the NVoc surface that were not exposed to light.

To explore further the concept of alignment marker and molecular glue functions within the same surface layer, the positively charged trimethylammonium silane and the NVoc silane were coadsorbed in two successive steps onto a silicon substrate. A mixed monolayer could be obtained also from simultaneous adsorption of a 1:1 mixture in solution. The exact ratio of ammonium versus NVoc silane in the monolayers is not clear at this point and is currently under investigation. Nevertheless, it can be proven that both functions, the cationic charge and the photolabile protecting group, both are present on the surface. When the mixed monolayer is irradiated through a mask and then immersed into the colloid suspension, the whole surface is covered with adsorbed particles, whereas the deprotected regions show a slightly higher surface coverage (Fig. 4*b*; irradiated region, 4.15 ± 0.78 particles per μm^2; protected areas, 2.67 ± 0.22 particles per μm^2). The particle adsorption can occur only in the presence of positive surface charges (compare Fig. 4*a*), confirming the incorporation of the ammonium silane. The slightly higher surface coverage on the irradiated areas supports the presence of NVoc functions. To validate the existence of the NVoc groups in the mixed monolayer, an irradiated substrate was treated with a fluorescence label (Alexa Flour 488) and imaged under a fluorescence microscope (Fig. 4*c*). As expected, only the deprotected regions reacted with the fluorescence label and appeared bright in the microscope. With these experiments, the possibility of incorporating functionalities in monolayers that control the selective adsorption of latex particles, along with photolabile moieties that allow chemical surface reactions after deprotection by light, could be explored successfully.

Discussion

From the above-described experiments we infer that complex surface morphologies can be generated by the regiospecific assembly of colloidal particles onto laterally structured silane monolayers. The required monolayer patterns can be obtained by a combination of the industrially well established photolithography process with the deposition of silanes from the vapor and liquid phase onto technologically highly relevant substrates such as silicon with an oxide layer, glass, and quartz. The regioselective particle adsorption, driven by electrostatic and polar interactions in combination with adhesion inhibition at hydrophobic surface layers, serves as a good model system for mesoscale object organization. The method is a self-controlled and highly parallel process that should allow the simultaneous fabrication of many devices in one assembly step with essentially no size limitations from nanometer to millimeter length scales.

The studied particle organization and positioning were found to be controlled by a complex interplay of different mechanisms such as electrostatic and hydrophilic versus hydrophobic interactions as well as interparticular capillary forces in combination with surface pinning of the adsorption liquid. The electrostatic interactions can be influenced by the pH of the aqueous environment, leading at low pH to protonation of the carboxylic acid functions on the particles. This effect in turn reduces the charge density and makes the particles more hydrophobic (ref. 21 and references therein and ref. 43), reducing the interparticlular distance at the surface (44). The situation is complicated further by the fact that the charge at opposing surfaces (such as COOH and SiOH) depends significantly on the separation between these surfaces (35). The particle density on patterned polyelectrolyte multilayers was shown also to be influenced by salt concentration or the presence of a surfactant (27) because of charge shielding (45–47).

Rearrangement of the electrostatically adsorbed particles caused by capillary forces during drying of the suspension liquid could be observed in accordance with the literature (25, 20). This effect was used to generate particle multilayers over specific silane layer regions, which might be developed into a fabrication process for patterned photonic bandgap structures on planar surfaces. The mobility of the electrostatically bound particles was lost after complete drying, suggesting a three-step mechanism for the particle adsorption. First, positioning and adhesion in the suspension liquid are controlled by charge and polar interactions between the substrate and particle surfaces. In the second step, capillary forces between the particles and the surface laterally displace the particles during drying. After complete evaporation in the third stage, an irreversible reorganization of the particle–substrate interface, which prevents resuspension or displacement when resubmerging the assembly into the adsorption liquid, must occur.

Many more factors influencing the particle–surface interactions such as surface topography and corrugation (48–52) or even nanoscopic air bubbles (53) might have to be taken into account. Concluding from this wealth of information, it might be very difficult to devise an analytical description or even a qualitative prediction of this very complex interaction scenario, and much more experimental and theoretical work in this direction is required before the concept of mesoscale object assembly can be implemented successfully in technological fabrication processes.

The integration of alignment marker molecules (to control object positioning) simultaneously with photoreactive functions as molecular glue (for permanent object fixation) within the same monolayer could be demonstrated by a two-step coadsorption of an ammonium silane and a photoprotected aminosilane. Future work may be directed toward the preparation of particles with activated surface functions (such as *N*-hydroxysuccinimide esters) that can react specifically with the deprotected aminosilane and thus complete the full cycle of object assembly and fixation after activation, as outlined in Fig. 1.

We thank Prof. Hans Wolfgang Spiess for his helpful discussions and continued support of this research. Furthermore, we thank Wacker Siltronic for the generous gift of the silicon wafers. Dr. Kenichi Morigaki is acknowledged for his support in fabricating the photolithography masks, and Uta Pawelzik for the latex preparation and dynamic light-scattering analysis. Financial support by the European Commission (Marie Curie Individual Fellowship for A.d.C.), Max Planck Society, Fonds der Chemischen Industrie, and Gesellschaft Deutscher Chemiker is highly appreciated.

1. Wallraff, G. M. & Hinsberg, W. D. (1999) *Chem. Rev.* (*Washington, D.C.*) **99,** 1801–1821.
2. Xia, Y., Rogers, J. A., Paul, K. E. & Whitesides, G. M. (1999) *Chem. Rev.* (*Washington, D.C.*) **99,** 1823–1848.
3. Cohn, M. B., Kim, C.-J. & Pisano A. P. (1991) in *IEEE Proceedings of the 6th International Conference on Solid-State Sensors and Actuators* (*Transducers '91*): *Digest of Technical Papers* (Cat. No.91CH2817–5), ed. Muller, R. S. (IEEE, New York), pp. 490–493.
4. Yeh, H.-J. H. & Smith, J. S. (1994) *Sensors Mater.* **6,** 319–332.
5. Hosokawa, K., Shimoyama, I. & Miura, H. (1996) *Sensors Actuators A* **57,** 117–125.
6. Bowden, N., Terford, A., Carbeck, J. & Whitesides, G. M. (1997) *Science* **276,** 233–235.
7. Tien, J., Terfort, A. & Whitesides, G. M. (1997) *Langmuir* **13,** 5349–5355.
8. Esener, S. C., Hartmann, D., Güncer, S., Fan, C., Heller, M. & Cable, J. (1997) in *Proceedings on Spatial Light Modulators, Topical Meeting, OSA Trends in Optics and Photonics Series*, ed. Fantone, S. D. (Opt. Soc. Am., Washington, D.C.) Vol. 14, pp. 65–68.
9. Srinivasan, U., Howe, R. T. & Liepmann, D. (1999) in *Proceedings on the International Conference on Solid-State Sensors and Actuators*, ed. Middelhoek, S. (Institute of Electrical Engineers of Japan, Sendai, Japan), pp. 1170–1173.
10. Nakakubo, T. & Shimoyama, I. (2000) *Sensors Actuators* **83,** 161–166.
11. Garcias, D. H., Tien, J., Breen, T. L., Hsu, C. & Whitesides, G. M. (2000) *Science* **289,** 1170–1172.
12. Öner, D. & McCarthy, T. J. (2000) *Langmuir* **16,** 7777–7782.
13. Hattori, H. (2001) *Adv. Mater.* **13,** 51–54.
14. Barthlott, W. & Neinhuis, C. (1997) *Planta* **202,** 1–8.
15. Craighead, H. G. (2000) *Science* **290,** 1532–1535.
16. Ehrfeld, W., Hessel, V. & Löwe, H. (2000) *Microreactors: New Technology for Modern Chemistry* (Wiley–VCH, Weinheim, Germany).
17. Effenhauser, C. S. (1999) in *Microsystem Technology in Chemistry and Life Sciences*, eds. Manz, A. & Becker, H. (Springer, Berlin), pp. 51–82.
18. Spichiger-Keller, U. E. (1998) *Chemical Sensors and Biosensors for Medical and Biological Applications* (Wiley–VCH, Weinheim, Germany).
19. Xia, Y., Gates, B., Yin, Y. & Lu, Y. (2000) *Adv. Mater.* **12,** 693–713.
20. Krüger, C., Spiess, H. W. & Jonas, U. (2001) *Proceedings PARTEC 2001: International Congress for Particle Technology* (VDI Gesellschaft, Düsseldorf, Germany) Vol. 17/2, pp. 1–8.
21. Tieke, B., Fulda, K.-F. & Kampes, A. (2001) in *Nano-Surface Chemistry*, ed. Rosoff, M. (Marcel–Dekker, New York), pp. 213–242.
22. Margel, S., Cohen, E., Dolitzky, Y. & Sivan, O. (1992) *J. Polym. Sci. Polym. Chem. Ed.* **30,** 1103–1110.
23. Slomkowski, S., Miksa, B., Trznadel, M., Kowalczyk, D. & Wang, F. W. (1996) *ACS Polym. Prep.* **37,** 747–748.
24. Taniguchi, T., Ohashi, T., Yamaguchi, K. & Nagai, K. (2000) *Macromol. Symp.* **151,** 529–534.
25. Aizenberg, J., Braun, P. V. & Wiltzius, P. (2000) *Phys. Rev. Lett.* **84,** 2997–3000.
26. Friebel, S., Aizenberg, J., Abad, S. & Wiltzius, P. (2000) *Appl. Phys. Lett.* **77,** 2406–2408.
27. Chen, K. M., Jiang, X., Kimerling, L. C. & Hammond, P. T. (2000) *Langmuir* **16,** 7825–7834.
28. Nakagawa, M., Oh, S.-K. & Ichimura, K. (2000) *Adv. Mater.* **12,** 403–407.
29. Krüger, C., Barrena, E. & Jonas, U. (2001) *Proceedings 1st European Silicon Days 2001* (Wacker-Chemie, Burghausen, Germany), in press.
30. Kleinfeld, D., Kahler, K. H. & Hockberger, P. E. (1988) *J. Neurosci.* **8,** 4098–4120.
31. Pillai, V. N. R. (1980) *Synthesis* (*Mass*), 1–26.
32. Effenberger, F. & Heid, S. (1995) *Synthesis* (*Mass*), 1126–1130.
33. Rai-Choudhury, P., ed. (1997) *Handbook of Microlithography, Micromachining, and Microfabrication* (SPIE Optical Engineering Press, Bellingham, WA).
34. Ulman, A., ed. (1995) *Organic Thin Films and Surfaces: Directions for the Nineties* (Academic, London).
35. Behrens, S. H. & Grier, D. G. (2001) *J. Chem. Phys.* **115,** 6716–6721.
36. Haller, I. (1978) *J. Am. Chem. Soc.* **100,** 8050–8055.
37. Kurth, D. & Bein, T. (1993) *Langmuir* **9,** 2965–2973.
38. Denkov, N. D., Velev, O. D., Kralchevsky, P. A., Ivanov, I. B., Yoshimura, H. & Nagayama, K. (1992) *Langmuir* **8,** 3183–3190.
39. Dushkin, C. D., Lazarov, G. S., Kotsev, S. N., Yoshimura, H. & Nagayama, K. (1999) *Colloid Polym. Sci.* **227,** 914–930.
40. McGall, G. H., Barone, A. D., Diggelmann, M., Fodor, S. P. A., Gentalen, E. & Ngo, N. (1997) *J. Am. Chem. Soc.* **119,** 5081–5090.
41. Fodor, S. P. A., Read, J. L., Pirrung, M. C., Stryer, L. T., Lu, A. & Solas, D. (1991) *Science* **251,** 767–773.
42. Vossmeyer, T., Jia, S., Delonno, E., Diehl, M. R., Kim, S.-H., Peng, X., Alivisatos, A. P. & Heath, J. R. (1998) *J. Appl. Phys.* **84,** 3664–3670.
43. Fulda, K. U. & Tieke, B. (1997) *Supramol. Sci.* **4,** 265–273.
44. Kampes, A. & Tieke B. (1999) *Mater. Sci. Eng. C* **8-9,** 195–204.
45. Russel, B., Saville, D. A. & Schowalter, W. R. (1989) *Colloidal Dispersions* (Cambridge Univ. Press, Cambridge, U.K.).
46. Witten, T. A. (1999) *Rev. Mod. Phys.* **71,** 367–373.
47. Giasson, S., Weitz, D. A. & Israelachvili, J. N. (1999) *Colloid Polym. Sci.* **277,** 403–413.
48. Van Blaaderen, A., Ruel, R. & Wiltzius, P. (1997) *Nature* (*London*) **385,** 321–324.
49. Lin, K.-h., Crocker, J. C., Prasad, V., Schofield, A., Weitz, D. A., Lubensky, T. C. & Yodh, A. G. (2000) *Phys. Rev. Lett.* **85,** 1770–1773.
50. Heni, M. & Löwen, H. (2000) *Phys. Rev. Lett.* **85,** 3668–3671.
51. Braun, P. V., Zehner, R. W., White, C. A., Weldon, M. K., Kloc, C., Patel, S. S. & Wiltzius, P. (2001) *Adv. Mater.* **13,** 721–724.
52. Lu, Y., Yin, Y. & Xia, Y. (2001) *Adv. Mater.* **13,** 34–37.
53. Tyrrell, J. W. G. & Attard, P. (2001) *Phys. Rev. Lett.* **87,** 1–4, no. 176104.